CrossMark

MOVPE growth of InAsBi/InAs/GaAs heterostructure analyzed by in situ spectral reflectance

R. Boussaha[1] · H. Fitouri[1] · A. Rebey[1] · B. El Jani[1]

Abstract InAsBi/InAs heterostructures were elaborated on semi-insulating GaAs substrate by atmospheric pressure metalorganic vapor phase epitaxy. Spectral reflectance in the range of 400–800 nm was employed to in situ monitor epitaxy. In order to determine optical constants of InAsBi films, an optical model incorporating two parameters: time-dependent surface roughness and time-dependent growth rate was established to simulate the in situ reflectance. Since bismuth has a crucial effect on surface kinetic mechanisms during growth of III–V semiconductors, a theoretical motivation introducing these two parameters instead of a standard single rms roughness and growth rate was provided. In order to evaluate the structural and optical properties of this material, reflectivity responses were analyzed for several wavelengths. Results were ex situ correlated with atomic force microscopy measurements.

1 Introduction

The addition of a small amount of bismuth in conventional III–V alloys leads to the formation of a new class of semiconductor compounds called 'dilute bismides'. In fact, they have been proposed as materials with a large band gap reduction and relatively temperature-insensitive band gap [1–3]. Therefore, it is possible to improve the high-temperature performance of optoelectronic devices such as uncooled long wavelength infrared photo-detectors

[4], lasers [5]. The synthesis of dilute bismides has been actively pursued with different growth techniques to take advantage of such properties [6–10]. The growth of such materials is very challenging and suffers from a large miscibility gap because the alloys are formed through isoelectronic substitution of group V elements with very different atomic sizes. That's why film morphology departs from homogeneity in several ways, including phase separation [11], atomic ordering [12] and surface-droplet formation [13]. Svensson et al. [14] have grown InAsBi/InAs layers by molecular beam epitaxy Photoluminescence (PL) characterization shows a local phase separation. Because of such phenomena, these materials have very particular growth processes which require more study. In situ techniques are helpful in order to follow the growth mechanism behavior and allow difficulty origin understanding. Spectral reflectance is one of powerful and elementary in situ monitoring epitaxy techniques for determining physical parameters of layers such as thickness, composition and optical refractive index.

In this paper, we present analysis of in situ spectral reflectance signals recorded during the metalorganic vapor phase epitaxy (MOVPE) of InAsBi/InAs/GaAs structure. An optical model incorporating time-dependent surface roughness and time-dependent growth rate was established to simulate reflectivity response. Transitory growth rate, surface roughness and optical constants are successfully determined for InAs and InAsBi.

2 Experimental procedure

InAsBi/InAs heterostructure was grown on semi-insulating GaAs substrate by atmospheric pressure MOVPEat a temperature of 375 °C. Trimethylbismuth (TMBi),

✉ A. Rebey
ahmed.rebey@fsm.rnu.tn

[1] Faculty of Sciences, Unité de Recherche sur les Hétéro-Epitaxies et Applications, University of Monastir, 5019 Monastir, Tunisia

trimethylinduim (TMIn) and pure arsine (AsH$_3$) were used as precursors. The substrate temperature was measured by a thermocouple inserted into the graphite susceptor. Before growth, substrate surface was cleaned by thermal desorption in presence of AsH$_3$ flow at 700 °C for 15 min in order to remove the native oxide. Then, growth temperature was decreased down and stabilized at the required value. Afterwards, an InAs buffer layer was grown for 2000s. Finally, TMBi was supplied to start InAsBi layer growth. The growth was monitored in situ by spectral reflectance (SR) technique. A halogen lamp was used as a light source, providing continuous spectral output from 380 to 2400 nm. Two optical fibers were used to carry the incident and the reflected beams, attached to the reactor windows under 30° angles with respect to the normal of the wafer surface. The reflected signal is detected by a spectrometer containing a charge coupled device (CCD). Then it is transferred to a personal computer. The experimental reflectivity signal (R) can be calculated as below:

$$R = 100 \times \left(\frac{R_{sample} - R_{dark}}{R_{reference} - R_{dark}} \right) \quad (1)$$

where R_{sample} is the reflected intensity of the studied system, $R_{reference}$ is the GaAs substrate reflectance measured at 375 °C prior the growth of InAs layer, and R_{dark} is the intensity measured when the incident light source is turned off.

3 Results and discussion

Figure 1 shows high-resolution X-ray diffraction (HRXRD) (004) ω-2θ curves for the InAsBi/InAs/GaAs heterostructure compared to InAs/GaAs sample. Two diffraction peaks are clearly resolved. However, the right narrow peak with a full width at half maximum (FWHM) of around 35 arcsec corresponds to the GaAs substrate. Other than substrate peak, a weak and wide peak located on its left side corresponds to the grown layer. Compared with the InAs pattern, the InAsBi related peak has a larger FWHM and a narrow shift at the lower-angle side shows low Bi incorporation. The Bi content in InAsBi heterostructure extracted from HRXRD measurements is about 1.4%. This value was estimated using Vegard's law by means of symmetric (004) and asymmetric (115) reflections ω/2θ measurements. The lattice constant of the hypothetical zinc blend InBi is assumed to be 7.024 Å [15]. Figure 2 presents the normalized experimental reflectivity, for a wavelength of 700 nm, as a function of growth time of InAsBi/InAs/GaAs heterostructure. The data in this plot is normalized to the growth temperature reflectivity just prior to InAs deposition following Eq. (1). After the annealing stage, the experience was started by the deposition of
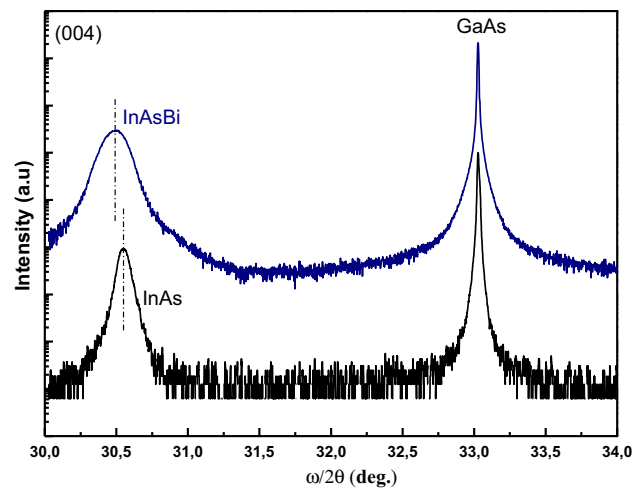

Fig. 1 High resolution X-ray diffraction (004) experimental ω/2θ curves of InAsBi/InAs/GaAs heterostructure and InAs/GaAs sample grown at the same growth parameters
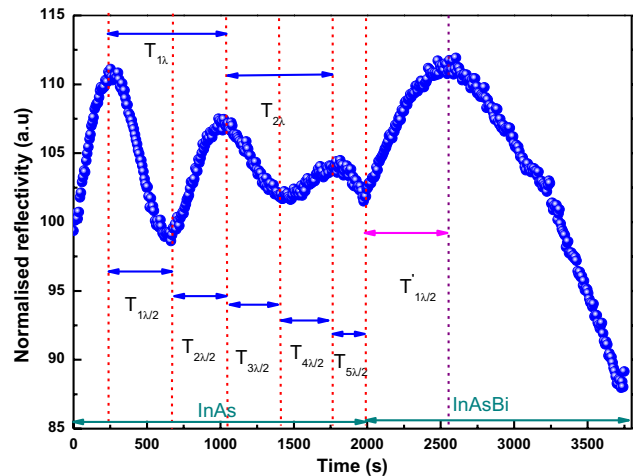

Fig. 2 Normalized experimental reflectivity response during process time of InAsBi/InAs/GaAs heterostructure growth for a wavelength of 700 nm. *Dashed lines* indicate the temporal positions of the extrema

InAs buffer layer followed by the active InAsBi one. When TMIn is introduced into the reactor, the reflectivity intensity shows different oscillations with different periods. This is due to the large lattice mismatch between InAs and GaAs, leading to the appearance of islands on the substrate surface in the first growth phase. These islands will grow and coalesce via a three-dimensional (3D) process. Then, dislocations with a high density are formed on the InAs relaxed surface layer at an advanced stage of growth. The transition from 3D to 2D growth mode causes a change in the absolute InAs growth rate (resulting from the contribution of lateral and vertical growth rates) as a function of time, and causes a particular

behavior in the recorded reflectivity oscillations. Moreover, reflectivity signal presents oscillations damping with deposition time. Any damping would result from roughness and/ or absorption coefficient of InAs for used wavelength [16]. Now, when TMBi is added to last mixture flow, reflectivity signal starts by an increase indicating a film formation with different refractive index from InAs buffer layer. After this increase, the reflectivity signal damps quickly due to the absorption coefficient of InAsBi layer at 700 nm and surface roughness effect which arises from a 3D nucleation and growth process. An accurate analysis of in situ reflectance shows a clear change in the growth rate between the two layers. This observation arises from the change in corresponding periods, since growth rate is defined as:

$$V_g = \frac{\lambda}{2n_\lambda T_\lambda \left(\cos\theta_r\right)_\lambda} \tag{2}$$

where $\lambda, n_\lambda, T_\lambda$ and $\left(\theta_r\right)_\lambda$ are the wavelength, the refractive index, the oscillation period and the refraction angle, respectively. Thus we clearly observe that InAsBi oscillation period is larger than that of InAs. It is known that using Bi as surfactant and/or incorporating element decreases the growth rate [17, 18]. So, compared to InAs, growing InAsBi exhibits lower growth rates. These observations will be subsequently confirmed by simulations and quantitative analysis.

In order to quantify these behaviors, we try to simulate the experimental data using recurrence method. We focus our attention on simultaneously extracting growth rates, roughness and optical constants for each stage. Breiland et al. [19] have developed an effective interface model for multi-layer structures with smooth interfaces to yield the refractive index of GaN layer and the growth rate from in situ reflectivity signal. This view is closely related to the concept of "equivalent layer". Hauge [20] showed how any multiple-layer film is the same as a single layer on an "effective substrate". For films grown with rough surfaces, quantitative analysis models have been developed to incorporate time-dependent surface roughness, and time-dependent growth rate, into the effective interface model. In our study, a quantitative optical model, including both time-dependent growth rate and time-depending surface roughness, has been successfully applied to simulate the reflectance evolution in order to determine the refractive index of InAsBi layer at growth temperature. Basing on Fresnel equations, for reflections from each smooth interface, and including the absorption properties of each layer through the imaginary part of its complex refractive index, we arrive at the following equations for the total complex reflection coefficient (r_m) in the two modes (s and p).

$$r_{ms} = \frac{r_{12s} + r_{234s}e^{-j\delta_2}}{1 + r_{12s}r_{234s}e^{-j\delta_2}}, \tag{3}$$

$$r_{mp} = \frac{r_{12p} + r_{234p}e^{-j\delta_2}}{1 + r_{12p}r_{234p}e^{-j\delta_2}} \tag{4}$$

where

$$r_{234s} = \frac{r_{23s} + r_{34s}e^{-j\delta_3}}{1 + r_{23s}r_{34s}e^{-j\delta_3}}, \tag{5}$$

$$r_{234p} = \frac{r_{23p} + r_{34p}e^{-j\delta_3}}{1 + r_{23p}r_{34p}e^{-j\delta_3}} \tag{6}$$

r_{234s} and r_{234p} re the reflection coefficient for the first stage of growth (InAs) in modes s and p respectively.

$$r_{12s} = \frac{N_1 cos\varphi_1 - N_2 cos\varphi_2}{N_1 cos\varphi_1 + N_2 cos\varphi_2} \tag{7}$$

$$r_{12p} = \frac{N_1 cos\varphi_2 - N_2 cos\varphi_1}{N_1 cos\varphi_2 + N_2 cos\varphi_1} \tag{8}$$

$$r_{23s} = \frac{N_2 cos\varphi_2 - N_3 cos\varphi_3}{N_2 cos\varphi_2 + N_3 cos\varphi_3} \tag{9}$$

$$r_{23p} = \frac{N_2 cos\varphi_3 - N_3 cos\varphi_2}{N_2 cos\varphi_3 + N_3 cos\varphi_2} \tag{10}$$

$$r_{34s} = \frac{N_3 cos\varphi_3 - N_4 cos\varphi_4}{N_3 cos\varphi_3 + N_4 cos\varphi_4} \tag{11}$$

$$r_{34p} = \frac{N_3 cos\varphi_4 - N_4 cos\varphi_3}{N_3 cos\varphi_4 + N_4 cos\varphi_3} \tag{12}$$

where r_{12s}, r_{12p}, r_{23s}, r_{23p}, r_{34s} and r_{34p} are Fresnel coefficients at interface vacuum/InAsBi, InAsBi/InAs and InAs/ substrate respectively. $\varphi_1 = \frac{\pi}{6}$ is the incidence angle and the successive refraction angles φ_i are defined by the following equation:

$$cos\varphi_i = \sqrt{1 - \left(\frac{n_{i-1}^2 + k_{i-1}^2}{n_i^2 - k_i^2}\right)\left(1 - cos^2\varphi_{i-1}\right)} \tag{13}$$

N_1, N_2, N_3 and N_4 are respectively the refractive index of vacuum, InAs buffer layer, InAsBi layer and GaAs substrate.

δ_i represents the phase change when light passes through layer i and is expressed by:

$$\delta_i = \frac{4\pi}{\lambda}N_i d_i cos\varphi_i \tag{14}$$

where N_i, d_i and $cos\varphi_i$ are the refractive index, the thickness and the refractive angle of i layer, respectively.

The effective Fresnel coefficients for the rough surface are defined by the equations below, in which the modifications factors are functions of $\sigma(t)$ (roughness profile).

$r'_{12} = r_{12}\alpha(t)$: r_{12} is the Fresnel reflection coefficient at the interface Ambient/Layer.

$r'_{21} = r_{21}\beta(t)$: r_{21} is the Fresnel reflection coefficient at the interface Layer/Ambient.

where

$$\alpha(t) = exp\left\{ -2\left[\frac{2\pi\sigma(t)}{\lambda}\right]^2 \right\} \quad (15)$$

$$\beta(t) = exp\left\{ -2\left[\frac{2\pi\sigma(t)}{\lambda}\right]^2 N_2^2 \right\} \quad (16)$$

$$\gamma(t) = exp\left\{ -\left(\frac{1}{2}\right)\left[\frac{2\pi\sigma(t)}{\lambda}\right]^2 \left(N_2^2 - N_1^2\right) \right\} \quad (17)$$

After these modifications, and by applying the traditional summation procedure, the complex reflectance amplitude for a rough surface has been obtained and expressed as below:

$$r'(t) = \frac{r_{12}\alpha(t) + r_{2s}\left[\gamma^2(t) + r_{21}^2\left(\alpha(t)\beta(t) - \gamma^2(t)\right)\right]exp\left(-\frac{i4\pi N_2 d(t)cos\varphi_i}{\lambda}\right)}{1 + r_{12}r_{2s}\beta(t)exp\left(-\frac{i4\pi N_2 d(t)cos\varphi_i}{\lambda}\right)} \quad (18)$$

The surface roughness profile $\sigma(t)$ is expressed as below:

$$\sigma(t) = \sigma_0 exp\left[\frac{t - t_i}{\alpha}\right]$$

where σ_0 is the initial surface roughness at the start time t_i, and α is the damping time of the layer.

It is well known that roughness sensitivity depends on the wavelength of the incident light. In most cases the presence of roughness handicaps the performance of devices except for solar cell which needs a textured surface in order to collect a maximum beam of sun light. There are some previous reports on estimating surface roughness and refractive index from reflection measurements with different methods [21–23]. In general, as one attempts to estimate several parameters simultaneously, the fits become less accurate. Note that growth rate under known growth conditions, can be determined previously based on earlier experiments [21]. In addition, a large spectral range of the incident beam is needed to investigate more precisely all parameters. For this purpose we have developed a numerical code using least square minimization which allows real time computation of a multilayer system reflectivity. The start point is to estimate input initial parameters. So, growth rate profile determined from oscillations periods and the refractive index of InAs as reported by Aspnes et al. [24] are introduced, initially, in order to determine iteratively the final results. The time-dependent relationship proposed

by Liu et al. [25] was used to model how the growth rate evolves as a function of growth time. The initial roughness is considered as a free fit parameter. Figure 3 presents the best fitting of the experimental reflectivity curves versus time for selected wavelengths: 400, 500, 550, 600, 700 and 800 nm, where the theoretical curves presented by continuous red line. A good agreement between experimental and simulated curves is seen. The evolutions of fitting parameters are reported in Fig. 4. The dependence of growth rate versus growth time could be associated to a morphology transition from 3D to 2D growth mode. For InAs layer the growth rate increases to reach its limit value as detailed in Fig. 4a. So we can subdivide it in two regimes, the first one is an increasing profile where the growth mode is 3D. Indeed due the large lattice mismatch between InAs layer and GaAs substrate (7%) [26], the first stage of the growth procedure is characterized by the presence of islands on the substrate surface (see the schematic drawing of the growth modes in the inset). These islands will grow and coalesce via a 3D process (as shown in Fig. 4a). Then InAs growth

rate reaches a limit value and remains constant, where the growth mode passes to a 2D mode. While InAsBi growth rate (Fig. 4b) has an increasing profile proving a 3D growth mode which can be attributed to the properties of bismuth atom. This earlier is characterized by strong surface segregation which promotes 3D growth mode. We note that InAsBi layer has a growth rate lower than that of InAs one. Qualitatively, this result is in good agreement with that reported by Ma et al. [27]. Quantitatively, our growth efficiency values are lower than those estimated in this last work. This difference can be attributed to the difference between the two used substrates. This growth rate reduction may be caused by the presence of bismuth into the reactor. Indeed, Bi changes significantly the interactions between mixture gaseous species and the solid surface giving rise to a surfactant effect or segregation phenomena. Similar effect was identified during growth of GaAsBi alloys [28, 29].

Figure 4c shows roughness profile during the two growth stages of InAs and InAsBi layers. We can see that the calculated roughness increases during time process. The evolution lines demonstrate that the last stage of growth is the most affected by roughness. Also, more the wavelength is low, more the roughness is high. Particularly, the sensitivity to the roughness becomes more important when the excitation wavelength decreases, and approaches the mean size of an island undulation describing the surface morphology. In fact, this observation is also supported by the low depth
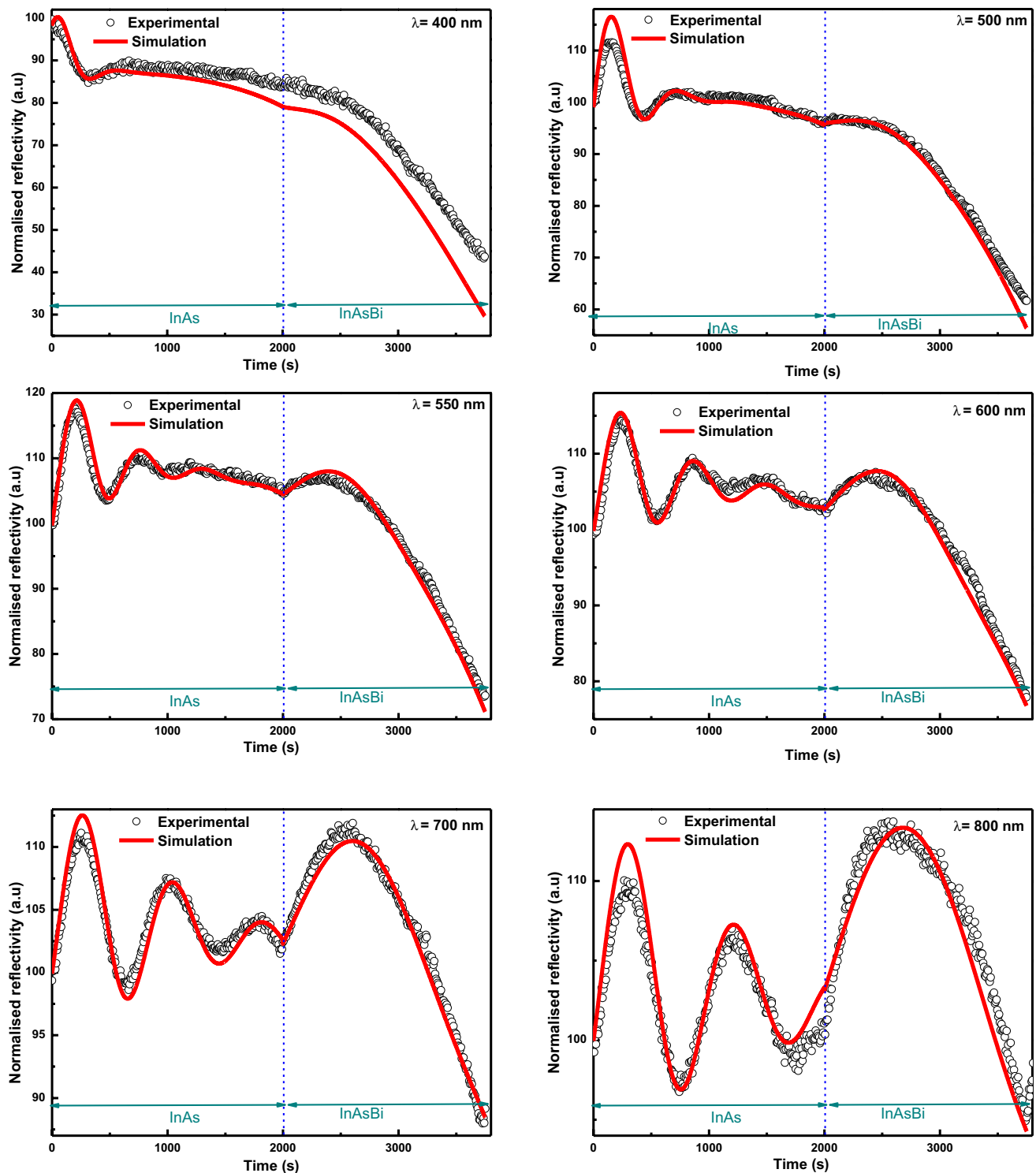
Fig. 3 The experimental (*squares*) and simulated (*solid line*) reflectance recorded during epitaxy of InAs/InAsBi layers for $\lambda = 400$, 500, 550, 600, 700 and 800 nm. *Dashed lines* indicate the temporal positions of InAsBi growth start

penetration of the incident beam which is inversely proportional to the absorption coefficient.

In order to correlate in situ roughness determined by simulation, and ex situ roughness determined by AFM

measurements, we present in Fig. 4d final roughness extracted from Fig. 4c as a function of wavelength compared to roughness value given by AFM. The mean value obtained from reflectivity (called optical roughness) is
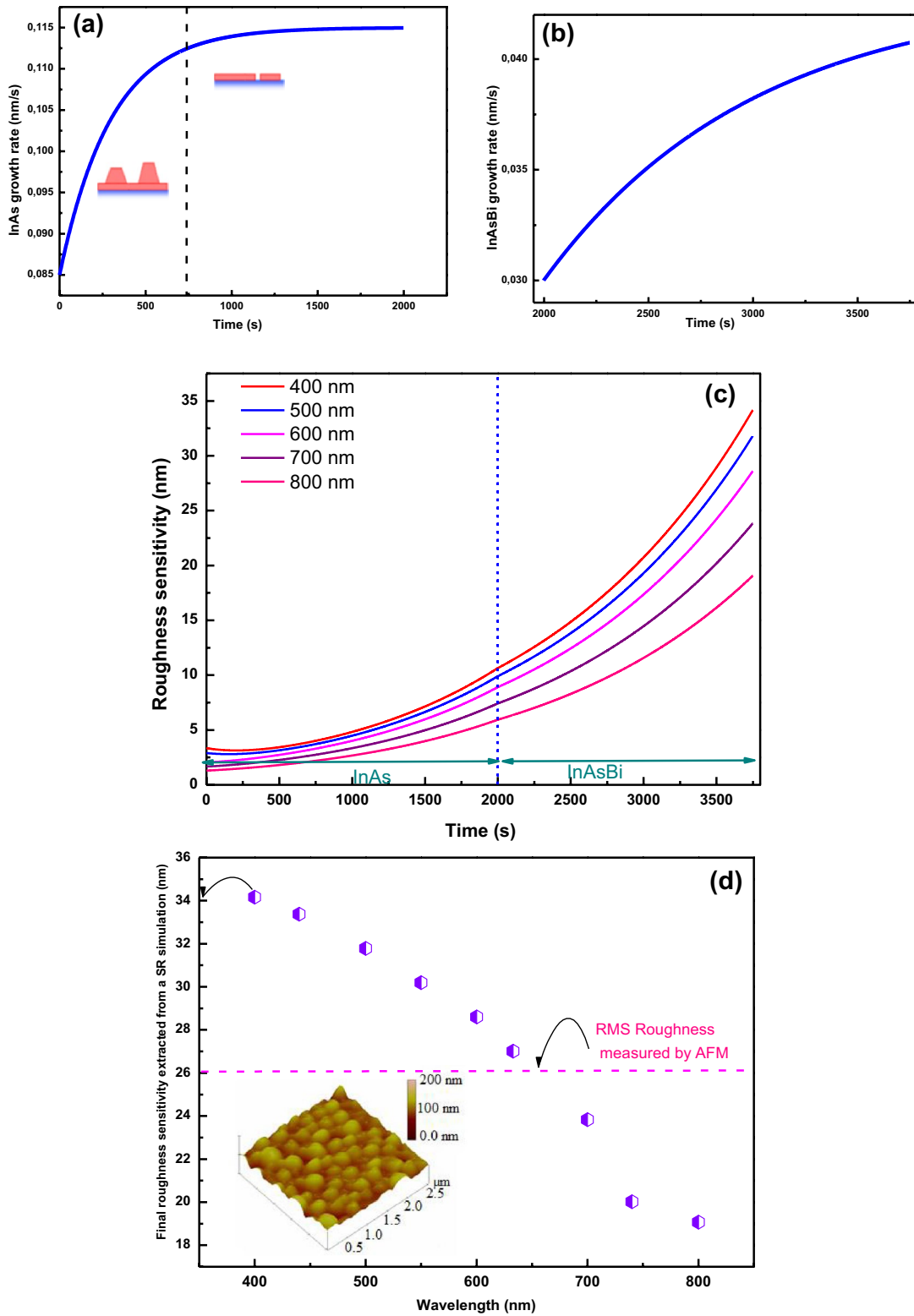
Fig. 4 Fitting parameters extracted from the best adjustment between experimental and theoretical reflectivity responses. **a** The growth rate of InAs. **b** The growth rate of InAsBi. **c** The variation of surface roughness sensitivity during growth of InAsBi/InAs heterostructure calculated for $\lambda = 400$, 500, 550, 600, 700 and 800 nm. **d** Extracted final surface roughness sensitivity values of InAsBi layer as a function of wavelength, the dotted line indicates the value of the RMS roughness measured by AFM

Fig. 5 Spectral dependence of refractive index (**a**) and extinction coefficient (**b**) of InAs material calculated in this work compared to that given by Aspnes et al. [23]
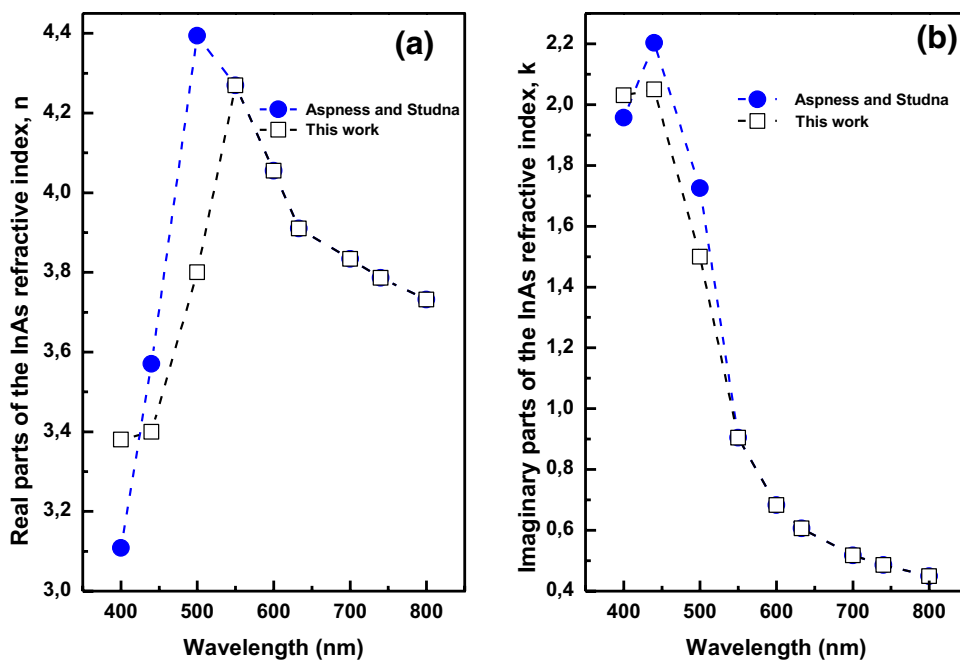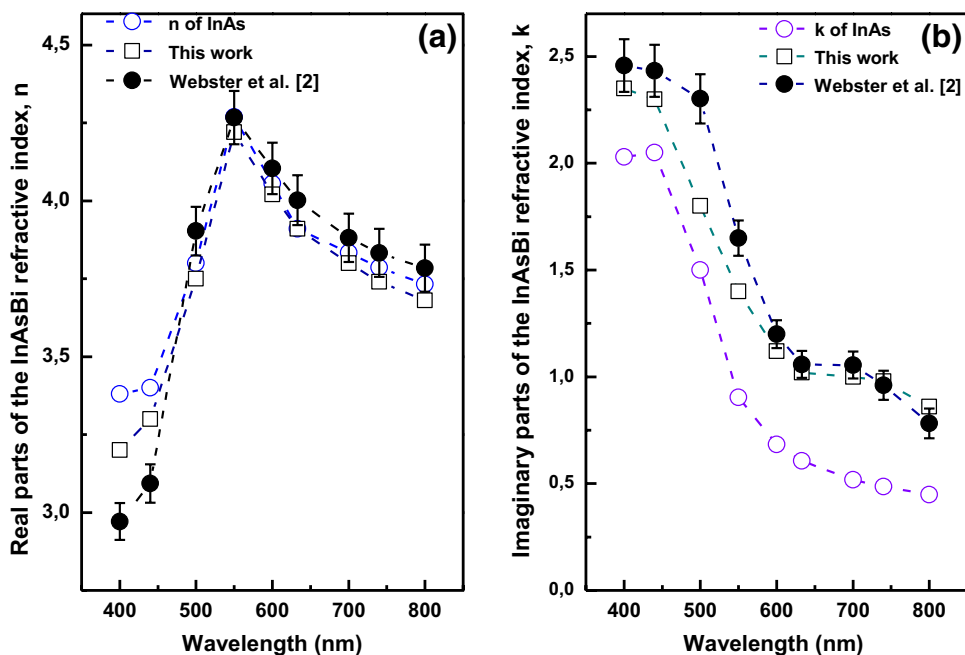

Fig. 6 Spectral dependence of refractive index (**a**) and extinction coefficient (**b**) of InAsBi layer calculated in this work compared to the InAs one and Webster et al. work

of about 27 nm. This value is in a good agreement with that deduced by ex situ AFM measurements. Zuiker et al. [30, 31] show that the root mean square (rms) surface roughness determined by in situ laser reflectometry is in a good agreement with ex situ AFM measurements for values under 60 nm. While others claim that it is generally difficult to expect a good agreement between the two

measurements [32]. Finally, let's focus on the refractive index of layers (InAs and InAsBi) as parameters used to successful reproduce experimental reflectivity signals. For InAs buffer layer, we have adopted the refractive index determined experimentally by Aspnes et al. [24] as a starting parameters in our simulation. Fitting results using these optical constants show bad reflectivity signal.

So, a correction in the refractive indices values is needed. Adjusted values deduced from reflectivity simulation are presented in Fig. 5. Note that InAs real part presents a maximum at 2.48 eV which correspond to the higher interband transition relative to the critical point E_1 [24]. Our results show that this value is shifted by -0.23 eV. This difference may be attributed to thermal effect on the band structure. Indeed, Massoudi et al. [33] found, for this critical point, a shift of -0.29 eV at a growth temperature of $450\,°C$. Unfortunately, less informations are available on optical constants of InAsBi. That's why we have used the refractive indices of InAs layer extracted from simulation as a starting parameters. Refractive index of InAsBi layer extracted from simulation are shown in Fig. 6 as a function of wavelength. These values are compared to those found for InAs, and bibliographic data of InAsBi [2]. It can be seen that the evolution of the refractive indices of InAsBi fitted curve has a similar behavior than that of InAs. However, the extinction coefficient of InAsBi is significantly higher than that of InAs. This results from the energy band gap reduction [4]. On the other hand, the real part maximum of InAsBi shows the same value as that of InAs with the same energy shift, indicating a similar sensitivity to the temperature variations. Comparing our results to bibliographic data [2], we can say that there is a good agreement in the real part variation. However there is a small difference in the imaginary part. This analysis reveals the variation of InAsBi band gap with Bi composition which can persists in imaginary part evolution. The high degree of correlation between optical data given by in situ analysis and those given by spectroscopic ellipsometry has been an ongoing challenge [21].

4 Conclusion

Spectral reflectance ranging from 400 to 800 nm is used to control MOVPE growth of InAs and InAsBi layers deposited on GaAs substrate. This technique is a powerful tool for monitoring thin-film growth. Real time in situ monitoring of reflectance provides a distinct interference oscillations giving helpful information about physical properties of elaborated material. Using our proposed model for spectral reflectance simulation, we have obtained the refractive index, the roughness and the growth rate profiles for each layer.

References

1. K.Y. Ma, Z.M. Fang, R.M. Cohen, G.B. Stringfellow, Ultra-low temperature OMVPE of InAs and InAsBi, J. Electron. Mater. **21**, 143 (1992)
2. P.T. Webster, A.J. Shalindar, N.A. Riordan, C. Gogineni, H. Liang, A.R. Sharma, S.R. Johnson, Optical properties of InAsBi and optimal designs of lattice-matched and strain-balanced III–V semiconductor superlattices. J. Appl. Phys. **119**, 225701 (2016)
3. P. Verma, K. Oe, M. Yamada, H. Harima, M. Herms, G. Irmer, Raman studies on $GaAs_{1-x}Bi_xGaAs_{1-x}Bi_x$ and $InAs_{1-x}Bi_x$. J. Appl. Phys. **89**, 1657 (2001)
4. I.C. Sandall, F. Bastiman, B. White, R. Richards, D. Mendes, J.P.R. David, C.H. Tan, Demonstration of InAsBi photoresponse beyond 3.5 μm. J. Appl. Phys. Lett. **104**, 171109 (2014)
5. I.P. Marko, P. Ludewig, Z.L. Bushell, S.R. Jin, K. Hild, Z. Batool et al., Physical properties and optimization of GaBiAs/(Al)GaAs based near-infrared laser diodes grown by MOVPE with up to 4.4% Bi. J. Phys D: Appl Phys. **47**, 345103 (2014)
6. J. Lu, P.T. Webster, S. Liu, Y.H. Zhang, S.R. Johnson, D.J. Smith, Investigation of MBE-grown InAs1–xBix alloys and Bi-mediated type-II superlattices by transmission electron microscopy. J. Cryst. Growth **425**, 250 (2015)
7. J. Lu, X.-H. Zhao, D.J. Smith, Y.-H. Zhang, S.R. Johnson, Molecular beam epitaxy using bismuth as a constituent in InAs and a surfactant in InAs/InAsSb superlattices, J. Vac. Sci. Technol. B **32**, 02C120 (2014)
8. K.T. Huang, C.T. Chiu, R.M. Cohen, G.B. Stringfellow, InAsBi alloys grown by organometallic vapor phase epitaxy. J. Cryst. Growth **134**, 29 (1993)
9. R. Boussaha, H. Fitouri, A. Rebey, B. El Jani, Effect of growth temperature and GaAs substrate misorientation on the morphology of InAsBi nanoislands grown by metalorganic vapor phase epitaxy. Appl. Surf. Sci. **291**, 40 (2014)
10. H. Fitouri, I. Moussa, A. Rebey, A. Fouzri, B. El Jani, AP-MOVPE of thin $GaAs_{1-x}Bi_x$ alloys. J. Cryst. Growth **295**, 114 (2006)
11. L. Dominguez, D.F. Reyes, F. Bastiman, D. L. Sales, R.D. Richards, D. Mendes, J.P.R. David, D. Gonzalez, Formation of tetragonal InBi clusters in InAsBi/InAs(100) heterostructures grown by molecular beam epitaxy. Appl. Phys. Express **6**, 112601 (2013)
12. D.P Samajdar, S. Dhar, Influence of Bi-related impurity states on the bandgap and spin–orbit splitting energy of dilute III–V-Bi alloys: $InP_{1-x}Bi_x$, $InAs_{1-x} Bi_x$, $InSb_{1-x} Bi_x$ and $GaSb_{1-x}Bi_x$. Superlattices Microstruct. **89**, 112 (2016)
13. G. Vardar, S.W. Paleg, M.V. Warren, M. Kang, R.S. Goldman, Mechanisms of droplet formation and Bi incorporation during molecular beam epitaxy of GaAsBi. Appl. Phys. Lett. **102**, 042106 (2013)
14. S.P. Svensson, H. Hier, W.L. Sarney, D. Donetsky, D. Wang, G. Belenky, Molecular beam epitaxy control and photoluminescence properties of InAsBi. J. Vac. Sci. Technol. B **30**, 02B109 (2012)
15. K.Y. Ma, Z.M. Fang, R.M. Cohen, G.B. Stringfellow, Organometallic vapor phase epitaxy growth and characterization of Bi containing III/V alloys. J. Appl. Phys. **68**, 4586 (1990)
16. M.M. Habchi, A. Rebey, A. Fouzri, B. El Jani, Laser reflectometry in situ monitoring of InGaAs grown by atmospheric pressure metalorganic vapour phase epitaxy. Appl. Surf. Sci. **253**, 275 (2006)
17. R.R. Wixom, L.W. Rieth, G.B. Stringfellow, Sb and Bi surfactant effects on homo-epitaxy of GaAs on (001) patterned substrates. J. Cryst. Growth **265**, 367 (2004)

18. I. Zaied, H. Fitouri, Z. Chine, A. Rebey, B. El Jani, Atmospheric-pressure metal-organic vapor-phase epitaxy of GaAsBi alloys on high-index GaAs substrates. J. Phys. Chem. Solids **75**, 244 (2014)

19. W.G. Breiland, K.P. Killeen, A virtual interface method for extracting growth rates and high temperature optical constants from thin semiconductor films using in situ normal incidence reflectance. J. Appl. Phys. **78**, 6726 (1995)

20. P.S. Hauge, Polycrystalline silicon film thickness measurement from analysis of visible reflectance spectra. J. Opt. Soc. Am. **69**, 1143 (1979)

21. I. Massoudi, M.M. Habchi, A. Rebey, B. El Jani, Study of surface roughness using spectral reflectance measurements recorded during the MOVPE of InAs/GaAs heterostructures. Physica. **E44**, 1282 (2012)

22. I. Massoudi, M.M. Habchi, A. Rebey, B. El Jani, Optical and morphological study of misoriented GaAs substrates exposed to bismuth flow using in situ spectral reflectance and atomic force microscopy. J. Cryst. Growth **353**, 77 (2012)

23. H. Fitouri, R. Boussaha, A. Rebey, B. El Jani, Oxidation of bismuth nanodroplets deposit on GaAs substrate, Appl. Phys. A. **112**, 701 (2013)

24. D.E. Aspnes, A.A. Studna, Dielectric functions and optical parameters of Si, Ge, GaP, GaAs, GaSb, InP, InAs, and InSb from 1.5 to 6.0 eV. Phys. Rev B. **27**, 985 (1983)

25. C. Liu, I.M. Watson, Quantitative simulation of in situ reflectance data from metal organic vapour phase epitaxy of GaN on sapphire. Semicond. Sci. Technol. **22**, 629 (2007)

26. Z.L. Miao, S.J. Chua, S. Tripathy, C.K. Chia, Y.H. Chye, P. Chen, High-quality InAs grown on GaAs substrate with an in situ micro-structured buffer. J. Cryst. Growth **268**, 18 (2004)

27. K.Y. Ma, Z.M. Fang, R.M. Cohen, G.B. Stringfellow, Investigation of organometallic vapor phase epitaxy of InAs and InAsBi at temperatures as low as 275 °C. J. Appl. Phys. **70**, 3940 (1991)

28. I. Moussa, H. Fitouri, A. Rebey, B. El Jani, Atmospheric-pressure metalorganic vapour phase epitaxy optimization of GaAsBi alloy. Thin Solid Films **516**, 8372 (2008)

29. A.J. Ptak, R. France, D.A. Beaton, K. Alberi, J. Simon, A. Mascarenhas, C.S. Jiang, Kinetically limited growth of GaAsBi by molecular-beam epitaxy. J. Cryst. Growth **338**, 107 (2012)

30. C.D. Zuiker, D.M. Gruen, A.R. Krauss, In situ laser reflectance interferometry measurement of diamond film growth. J. Appl. Phys. **79**, 3541 (1996)

31. C.D. Zuiker, D.M. Gruen, A.R. Krauss, Laser-reflectance interferometry measurement of diamond-film growth, MRS Bull. **20**, 29 (1995)

32. D. Franta, I. Ohlidal, Comparison of effective medium approximation and Rayleigh–Rice theory concerning ellipsometric characterization of rough surfaces. Opt. Commun. **248**, 459 (2005)

33. I. Massoudi, M.M. Habchi, A. Rebey, B. El Jani, In situ spectral reflectance investigation of InAs/GaAs heterostructures grown by MOVPE. J. Electron. Mater. **41**, 498 (2012)